Supporting Information

Stable Multimetallic Nanoparticles for Oxygen Electrocatalysis

Steven D. Lacey[1‡], Qi Dong[2‡], Zhennan Huang[3], Jingru Luo[2], Hua Xie[1], Zhiwei Lin[1], Dylan J. Kirsch[1], Vivek Vattipalli[4], Christopher Povinelli[2], Wei Fan[4], Reza Shahbazian-Yassar[3], Dunwei Wang[2], Liangbing Hu[1*]*

[1]Department of Materials Science and Engineering, University of Maryland, College Park, MD 20742, USA.

[2]Department of Chemistry, Boston College, Chestnut Hill, MA 02467, USA.

[3]Department of Mechanical and Industrial Engineering, University of Illinois at Chicago (UIC), Chicago, IL 60607, USA.

[4]Department of Chemical Engineering, University of Massachusetts, Amherst, MA 01003, USA

Correspondence: binghu@umd.edu[*] (L.H.); dunwei.wang@bc.edu[*] (D.W.)

[‡]These authors contributed equally to this work

Experimental Methods

Starting Materials and Synthesis: Lithium bis(trifluoromethane)sulfonimide (LiTFSI, ≥99.95%, trace metals basis), 1,2-dimethoxyethane (DME, anhydrous), lithium ribbon (≥ 99.9%, trace metals basis, 0.38 mm) and polytetrafluoroethylene (PTFE, 60 wt.% aq.) were all purchased from Sigma-Aldrich. DME was further dried with 4 Å molecular sieves prior to cell assembly. Deionized water (DI H_2O, 18.2 MΩ•cm) was obtained with a Barnstead Nanopure Diamond system. The DME-based electrolyte was prepared by dissolving 1 M LiTFSI into the dried DME. The water-in-salt (WiS) electrolyte was prepared by dissolving 21 m (21 mole per 1 kg) LiTFSI into DI H_2O. Carbon paper (Toray 120) gas diffusion layers were purchased from the Fuel Cell Store, cleaned in sequence with acetone, methanol and isopropanol, and then thoroughly dried under vacuum before use. Three-dimensionally ordered mesoporous (3DOm) carbon was prepared using similar processes reported by Fan *et al.*[1], where colloidal silica nanoparticle assemblies act as templates to promote controlled pore size formation. The interconnected spherical pores (ca. 35 nm) were created by sintering the silica nanoparticles and infiltrating the assembly with curable polymers. A carbonization step followed by removal of the silica nanoparticle template (dissolving in an alkaline solution) yields the porous carbon replica (i.e. 3DOm carbon), which resembles an inverse FCC close-packed structure. Vulcan XC72 carbon black was purchased from Cabot Corporation. $LiFePO_4$ (LFP, active material density: 120 g m^{-2}, single sided) was purchased from MTI. Similar to a previous study[2], the LFP films were cut into square pieces (area of ca. 1.5 cm^2) and acted as both the pseudo-counter electrode and reference electrode within the WiS electrolyte platform.

Preparation of Carbon-Loaded Carbon Paper and CTS Device: 3DOm or Vulcan carbon with PTFE binder was dispersed in isopropyl alcohol (IPA) in a 95:5 mass ratio. The prepared solution was then diluted in order to achieve a specific weight loading (1.0 ± 0.1 mg) on the clean carbon paper through repeated drop casting steps. The cathode substrate has an area size of ca. 1.0 cm^2, therefore yielding a loading density of ca. 1.0 mg cm^{-2}. The conformal coverage

by carbon powders was confirmed by SEM before testing. The electrodes were further dried in a vacuum oven for 2 days at 140 ºC to remove any residual solvents. To prepare the CTS device, the carbon-loaded carbon paper substrates were cut in half (ca. 1 cm × 0.55 cm) and attached to the custom device platform used to apply current (i.e. electrical pulse) via the CTS method in an Ar-filled atmosphere. Specifically, the carbon-loaded supports were suspended between glass slides, where copper electrodes and silver paste provided the electrical connections as reported previously by our group.[3]

Synthesis of Solid Solution Catalysts via CTS and WI: All samples reported in this work were prepared using ethanol-based precursor solutions (varied between 0.05 M and 0.10 M; optimized at 0.05 M), as ethanol exhibits better wettability with carbon and therefore, enables more uniform dispersions. The solutions were directly dropped onto the suspended carbon-loaded supports with the desired precursor loading (varied between 20 and 240 μL cm^{-2}; optimized at 120 μL cm^{-2}) and left to dry at room temperature. Note that the elemental precursor solutions were first combined together in the desired volume ratio to create mixed binary, ternary, quaternary or octonary compositions prior to drop casting. The ternary and quaternary compositions reported herein used a total of 10 vol% of 3rd and 4th elements, with the same RuIr ratio (Ru-rich). The octonary compositions reported herein used a total of 24 vol% for the catalytically inert elements, also with the same RuIr ratio. The CTS process was achieved by electrically-triggered Joule heating of the precursor-loaded carbon supports in an Ar-filled glovebox. Due to the low resistance (<1 Ω) of the aforementioned carbon supports, a high current/voltage regulated DC power supply (VOLTEQ HY6020EX) acted as the external power source with an adjustable current range up to 20 A. A high current electrical pulse was applied directly to the carbon-loaded supports in an Ar-filled glovebox to induce a ≤1 s thermal shock. Due to the defect density of the carbon-loaded supports, multimetallic (solid solution) nanoparticles with diameters on the order of nanometers can be reproducibly produced using a ≤1 s shock duration. The WI method utilizes the same precursor loading procedure described

above however, thermal reduction occurs in a tube furnace under a constant Ar flow (80 mL/min) using the following parameters: 5°C/min ramp from RT to 500°C, hold for 2h, and then cool down naturally.

Electrochemical Measurements: All electrochemical tests were carried out with a VMP3 potentiostat (BioLogic) using a home-designed Swagelok-type cell described previously[4]. The electrochemical measurements were conducted in an Ar-filled/O_2-tolerant glovebox (Mbraun, H_2O <0.1ppm) at room temperature. The Li-O_2 testing cells were fabricated using a 2-electrode configuration. The catalyst-decorated Vulcan or 3DOm carbon loaded supports were used directly as the cathode, with an area of ca. 0.5 cm^2 after the CTS (or WI) process. Lithium ribbon (area of ca. 1 cm^2) was used as the anode. Two pieces of polypropylene separators were used to separate the respective electrodes. Note that two pieces of glass microfiber (GF/F, Whatman) separators were used for the WiS electrolyte. All current density and capacity values were normalized to the applied weight of the 3DOm or Vulcan carbon. In a typical experiment, 100 µL DME-based electrolyte or 250 µL WiS electrolyte was applied to each Li-O_2 cell. After assembly, ultra-high purity O_2 (Airgas) was purged through the head space of the Swagelok cell at 20 sccm for at least 1 minute. The cell was then separated from the O_2 line afterwards when the pressure equilibrated to 760 torr. The rate measurements for the 3DOm carbon cathodes were conducted at 200 mA g_{carbon}^{-1} and 500 mA g_{carbon}^{-1} for each catalyst composition with a cutoff capacity of 250 mAh g_{carbon}^{-1}. Accordingly, the galvanostatic cycling tests with DME-based electrolyte were conducted at a current density of 200 mA g_{carbon}^{-1} with a cutoff capacity of 500 mAh g_{carbon}^{-1} (operated for 5 h per cycle). For the WiS electrolyte, Vulcan carbon cathodes were tested against an LFP pseudo-anode at 50 mA g_{carbon}^{-1} with a cutoff capacity of 250 mAh g_{carbon}^{-1} (operated for 10 h per cycle). Note that the total capacity of the Li or LFP pseudo-anode was in excess compared to the applied capacities for all electrochemical measurements.

Material Characterization: Before spectroscopic and microscopic post-characterization, the carbon-based cathodes were operated at 200 mA g_{carbon}^{-1} in order to reach either a cutoff of 500 mAh g_{carbon}^{-1} or the fully discharged state. The electrode samples were then collected in an Ar-filled/O_2-tolerant glovebox (Mbraun, H_2O <0.1 ppm), washed with DME at least 5 times to remove remaining residues, and then dried under vacuum for 6 hrs. X-ray photoelectron spectroscopy (XPS) was conducted on a Thermo Scientific K-Alpha system with an Al X-ray source (incident photon energy: 1486.7 eV). The fitting of XPS data was carried out using XPS Peak 4.1 software. Scanning electron microscopy (SEM) was performed using a JEOL 6340F microscope with a 10 kV accelerating voltage. Both SEM and XPS samples were carefully transported to their respective characterization tools using sealed Ar-filled bags. The samples were then mounted onto the stage with a short exposure to air (<5 min) before entering the high vacuum chamber. The TEM samples were prepared by first sonicating the cathode samples in ethanol to disperse the carbon powders in an Ar-filled vial, then drop cast onto the TEM grid. The HRTEM and HAADF images were captured at 200 kV inside a JEOL JEM-ARM 200CF. The HAADF images were captured using a 90 mrad inner-detector angle. The X-ray energy dispersive spectroscopy (EDS) analysis was performed with an Oxford X-max 100TLE windowless SDD X-ray detector with a resolution of 512 and a pixel dwell time of 50 μs. The Ru content within the synthesized catalysts were quantified using inductively coupled plasma optical emission spectrometry (ICP-OES). The mass loading of Ru was measured to be ca. 0.1 mg cm^{-2}.

1. Characterization of 3DOm carbon

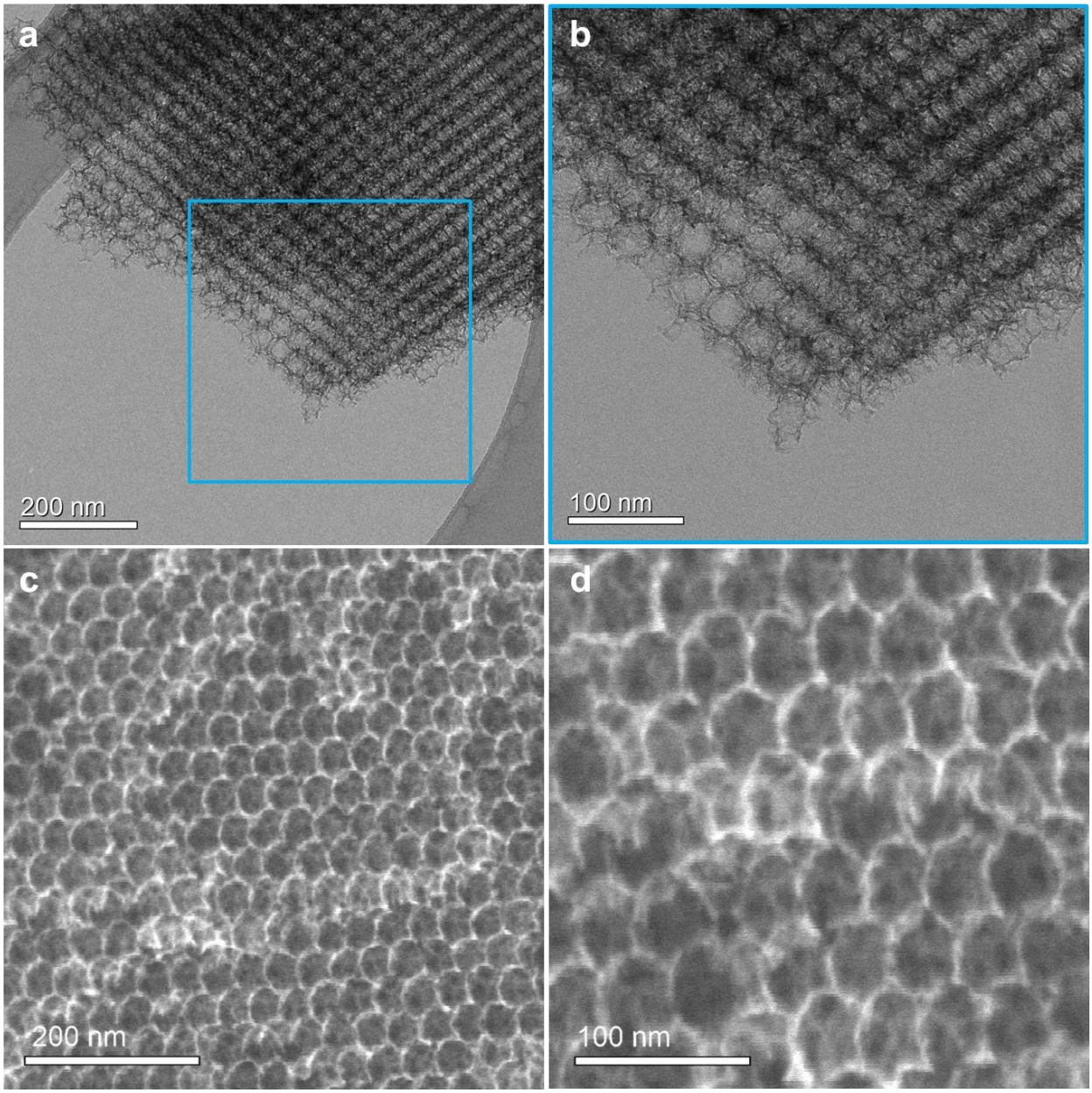

Figure S1. (a-b) TEM and (c-d) SEM images of the mesoporous 3DOm carbon, where through-pores on the order of tens of nanometers (ca. 35 nm) are present.

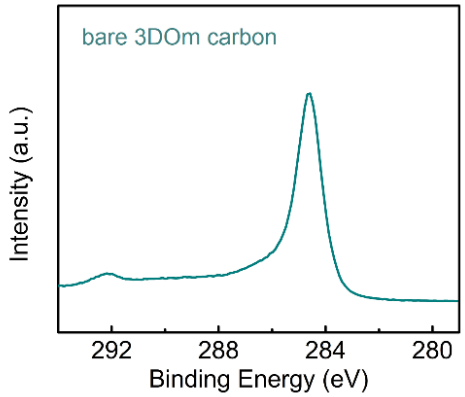

Figure S2. The C 1s XPS spectrum of the pristine 3DOm carbon cathode before loading electrocatalysts. Note the peak around 292 eV represents PTFE binder.

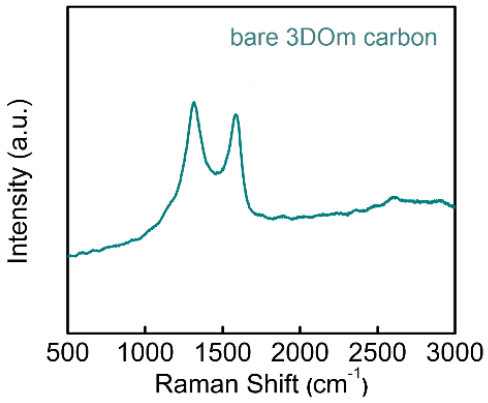

Figure S3. The Raman spectrum of the pristine 3DOm carbon before loading electrocatalysts. The prominent D band is indicative of the defective nature of the 3DOm carbon.

2. Comparison between bimetallic and/or monometallic compositions during Li-O_2 battery operation

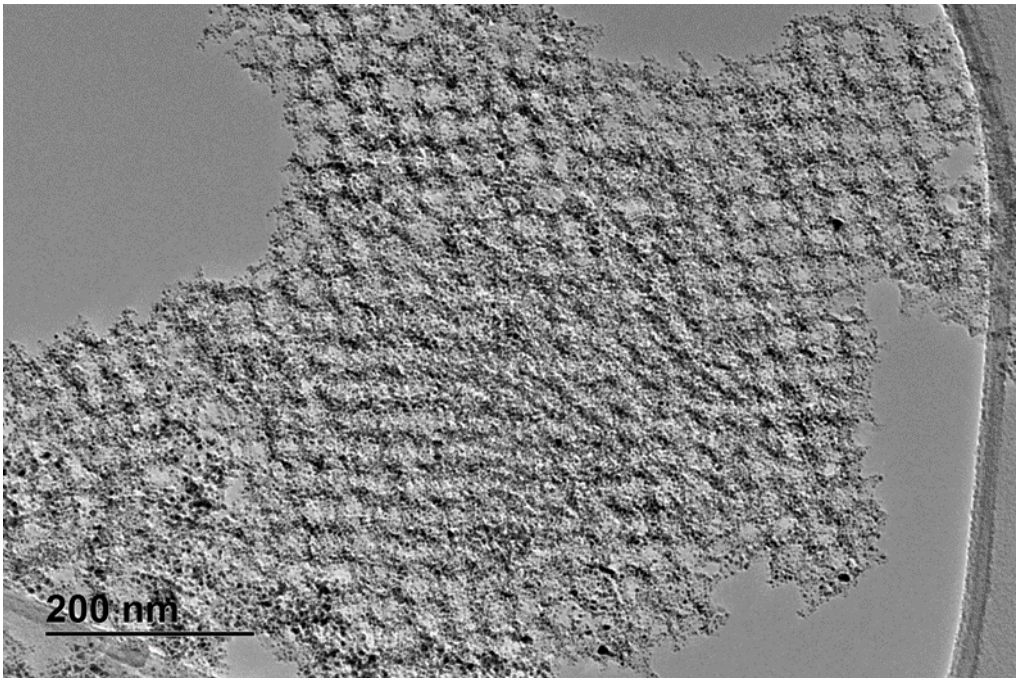

Figure S4. TEM image of the mesoporous 3DOm carbon evenly decorated with 2-3 nm RuIr nanoparticles after CTS synthesis. Note the rapid electrically-triggered thermal shock via CTS preserves the ordered structure as well as the inherent porosity of the carbon support.

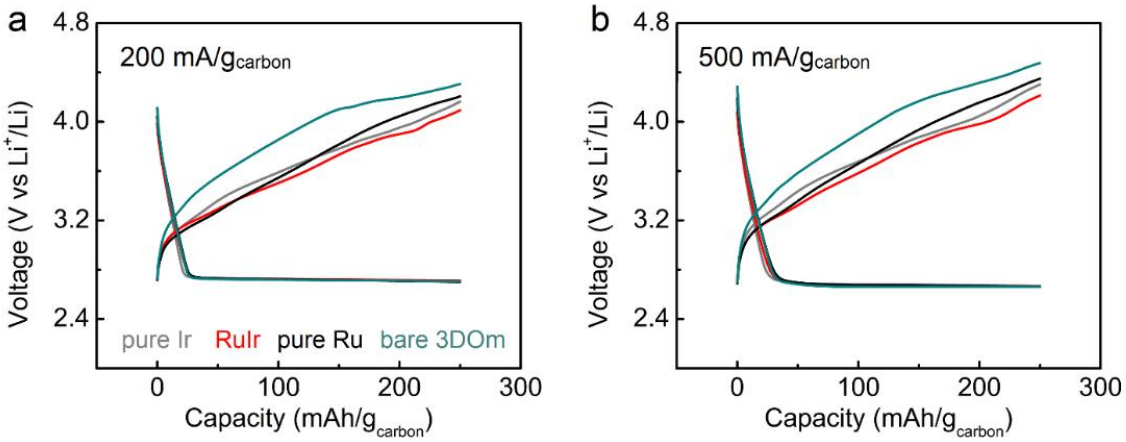

Figure S5. Comparison of electrocatalytic performance between monometallic (Ru or Ir) and bimetallic (RuIr) nanoparticle-loaded Li-O_2 cathodes using 3DOm carbon as the substrate. Note the cells were tested at two current densities: (a) 200 mA/g_{carbon} and (b) 500 mA/g_{carbon}.

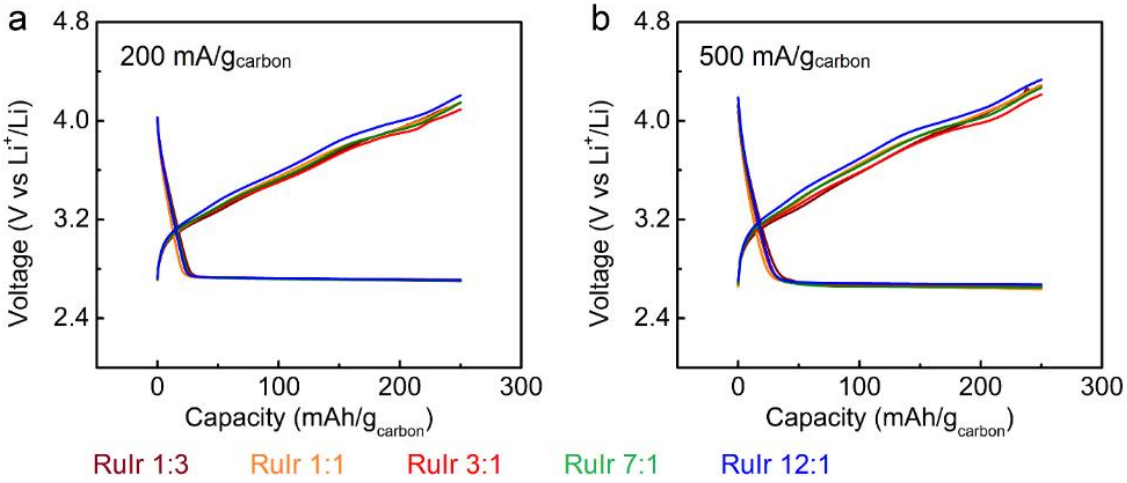

Figure S6. Electrocatalytic performance comparison between numerous bimetallic (RuIr) compositions on 3DOm carbon supports. In Li-O_2 battery cells, each RuIr ratio (by precursor volume) exhibits similar overpotentials and terminal potentials at both current densities: (a) 200 mA/g_{carbon} and (b) 500 mA/g_{carbon}.

3. Application of CTS nanoparticles on Vulcan carbon substrates

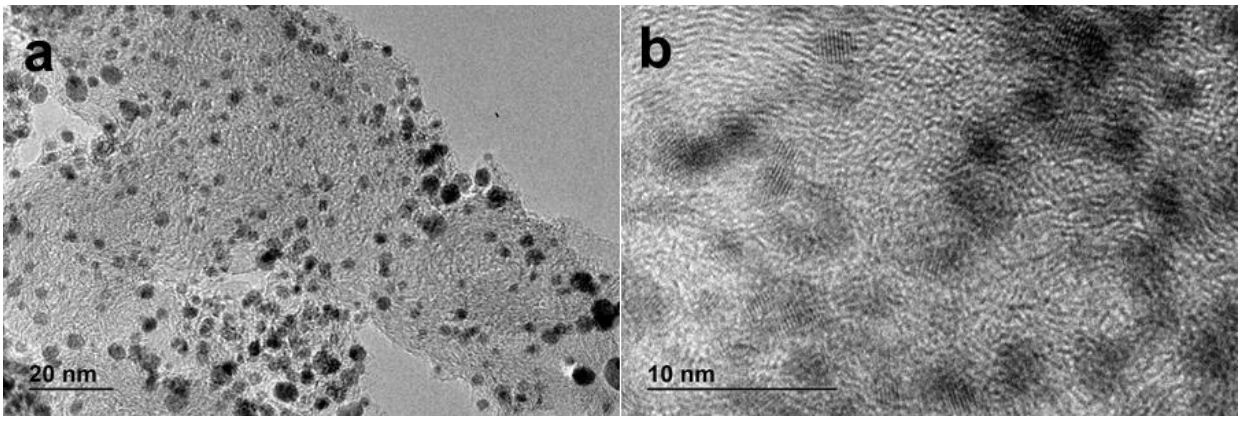

Figure S7. (a-b) TEM images of RuIr compositions on commercial Vulcan carbon using the same CTS parameters.

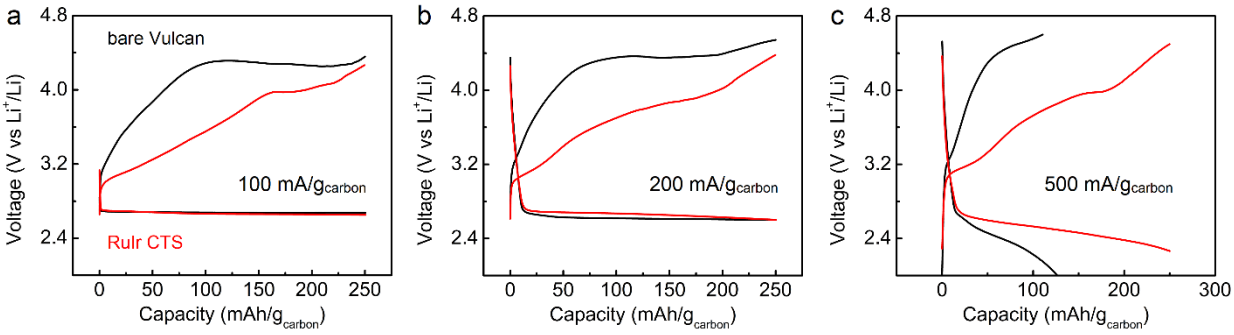

Figure S8. (a-c) The electrocatalytic performance of the same bimetallic RuIr nanoparticle composition loaded onto a different cathode support (i.e. Vulcan carbon) compared to the bare support. The Li-O_2 battery cells were tested at three current densities (100 mA/g_{carbon}, 200 mA/g_{carbon} and 500 mA/g_{carbon}), where the nanoparticle-loaded Vulcan cathodes showed much improved performance compared to the bare Vulcan cathode.

4. Control experiment to verify no changes occur to 3DOm carbon during furnace treatment

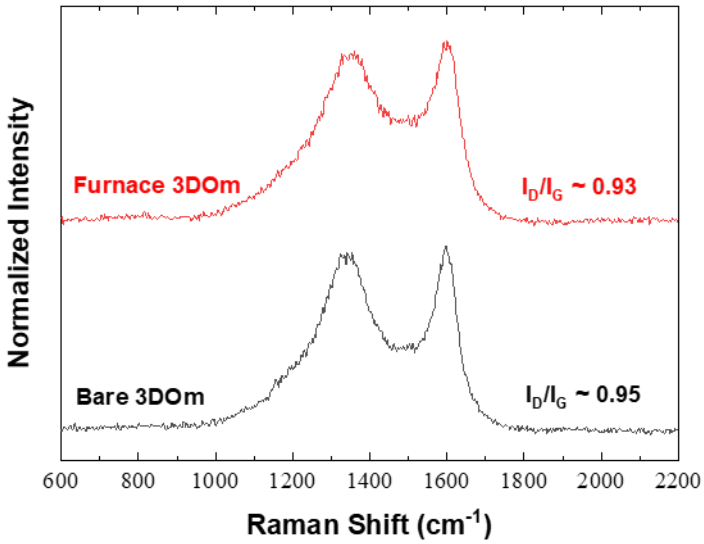

Figure S9. Raman spectra for a bare 3DOm support and one after thermal treatment in a tube furnace. Note that the furnace treatment parameters used here are identical to the ones used to prepare the WI samples, however, no metal salt precursors were loaded beforehand. The defect level of 3DOm supports before and after furnace treatment is essentially unchanged according to the near identical I_D/I_G ratios.

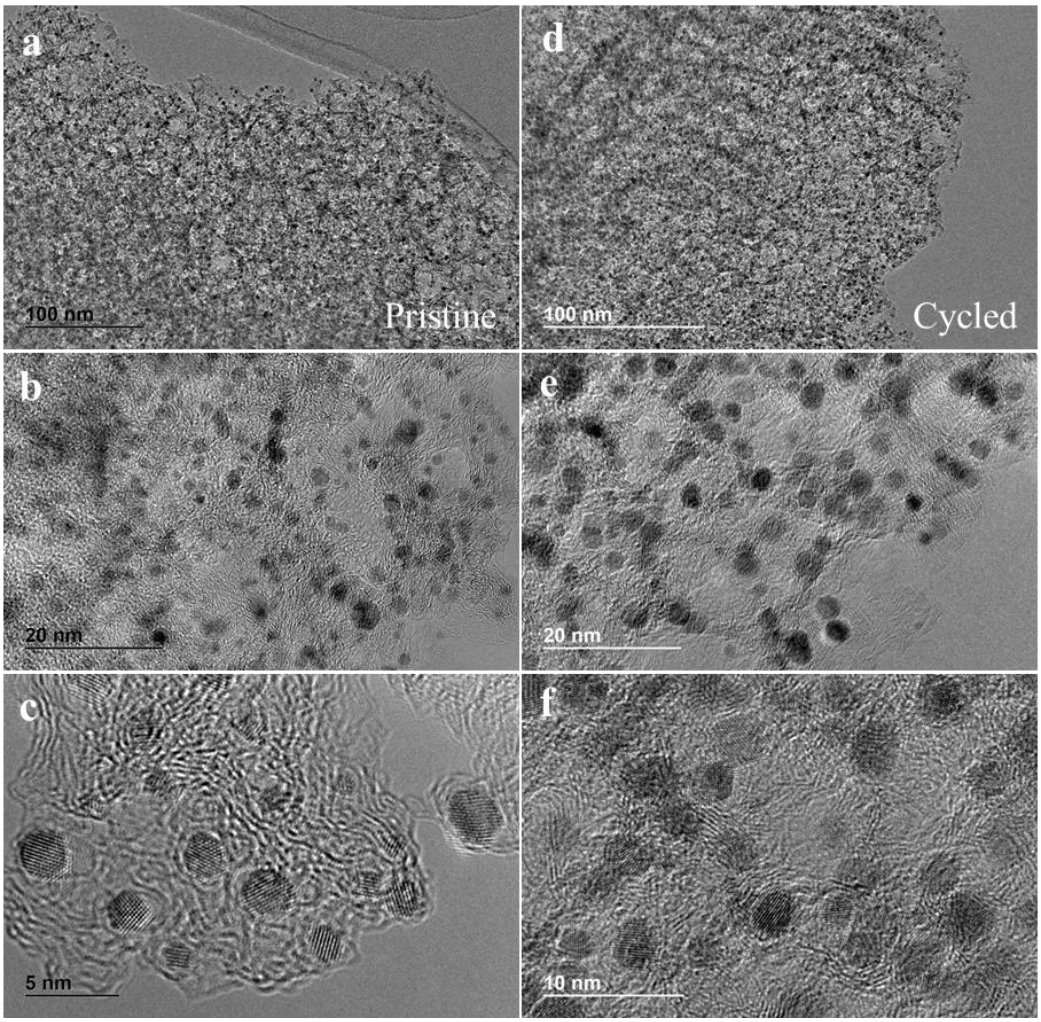

Figure S10. Characteristic TEM images of the furnace+CTS treated RuIr/3DOm cathodes (a-c) before and (d-f) after electrochemical cycling in aprotic Li-O_2 test cells. No obvious changes in terms of particle size or dispersion are evident, which corroborates our hypothesis regarding the CTS method facilitating enhanced catalytic stability.

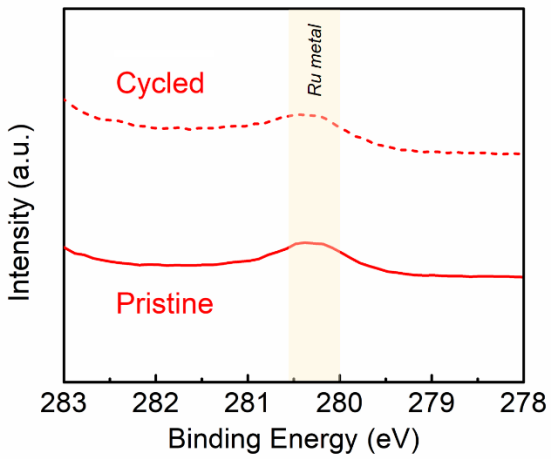

Figure S11. XPS Ru 3d spectra of the pristine and cycled furnace+CTS treated RuIr/3DOm cathodes. The curves indicate that the Ru content of the synthesized nanoparticles both before and after electrochemical testing remain metallic in nature.

5. Comparison between CTS and WI bimetallic nanoparticles as Li-O_2 battery electrocatalysts

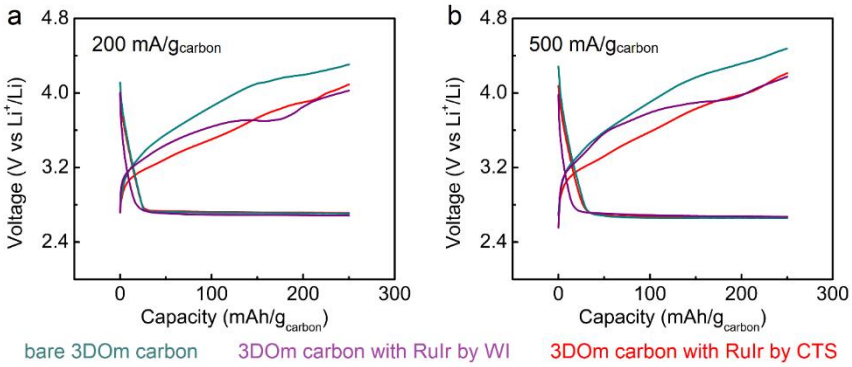

Figure S12. Electrocatalytic performance comparison between CTS and WI bimetallic (RuIr) nanoparticles on 3DOm carbon as well as the bare 3DOm Li-O_2 battery cathode. The cells were tested at two current densities: (a) 200 mA/g_{carbon} and (b) 500 mA/g_{carbon}.

6. Morphology of ternary and quaternary CTS nanoparticles on 3DOm carbon substrates

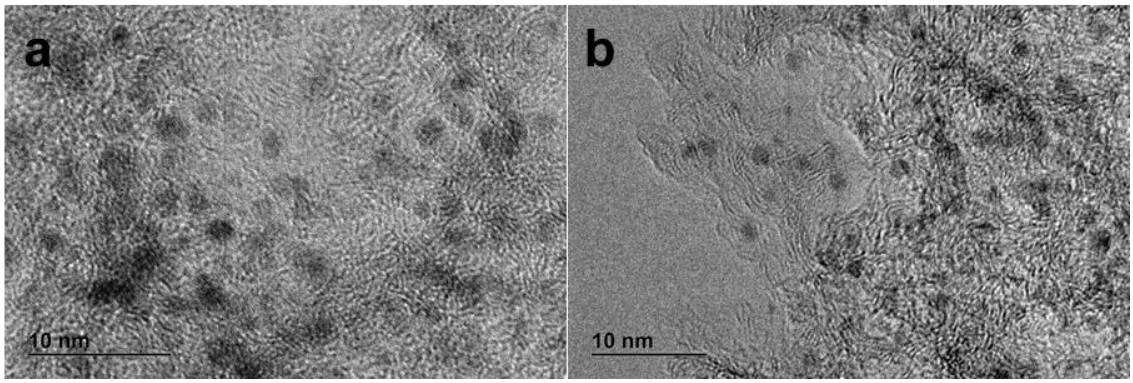

Figure S13. (a-b) TEM images of ternary RuIrNi nanoparticles evenly dispersed on 3DOm carbon.

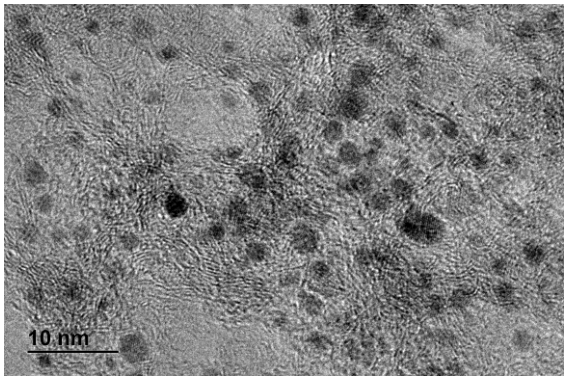

Figure S14. TEM image of the 4-element composition (RuIrCeNi) on 3DOm carbon with 2-3 nm nanoparticle diameters.

7. Elemental maps of quaternary and octonary CTS nanoparticles on 3DOm carbon substrates

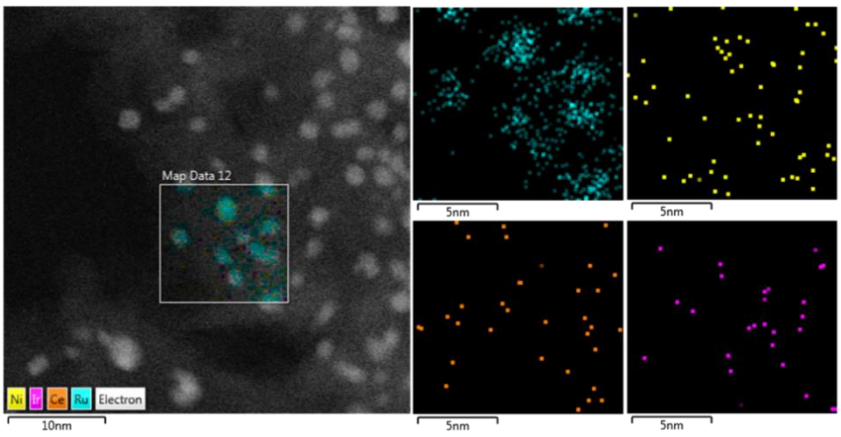

Figure S15. Overlay and individual elemental maps for the as-synthesized RuIrCeNi nanoparticles on 3DOm.

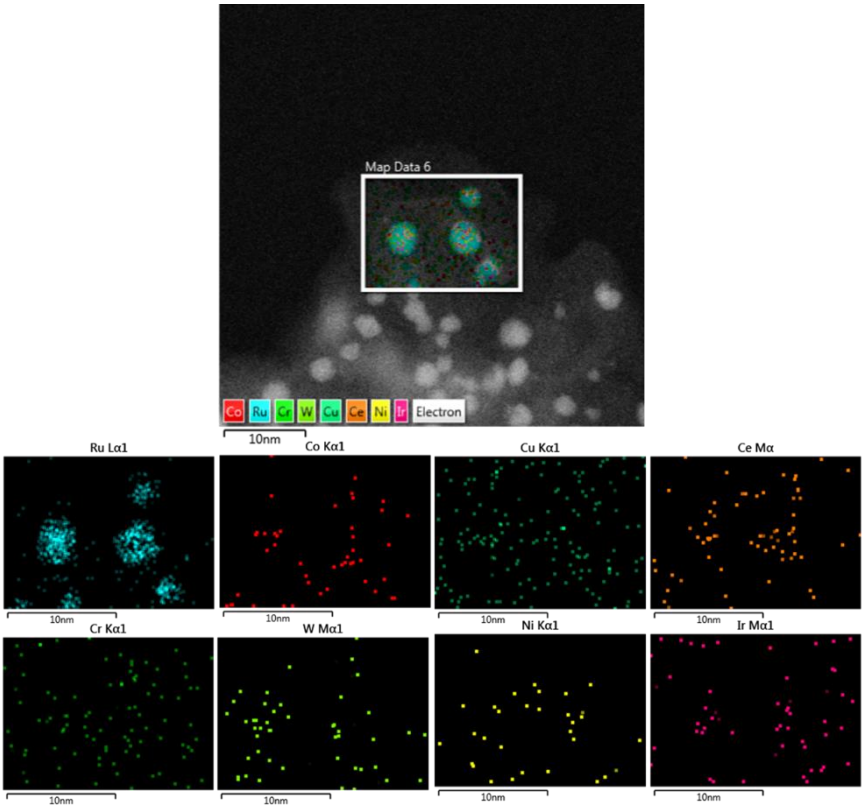

Figure S16. Overlay and individual elemental maps for the as-synthesized 8-element (RuIrCeNiWCuCrCo) CTS nanoparticles on 3DOm.

8. Comparison of the electrocatalytic performance among binary, ternary, quaternary and octonary CTS-synthesized nanoparticles using Li-O_2 battery cells

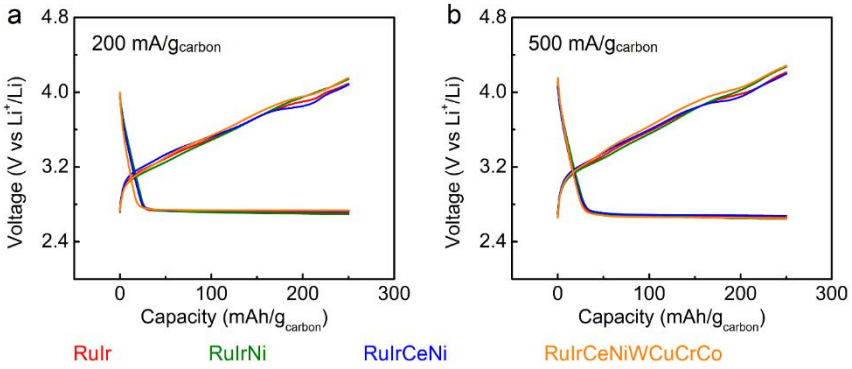

Figure S17. Electrocatalytic performance of binary (red), ternary (green), quaternary (blue) and octonary (orange) nanoparticles on 3DOm carbon cathodes. Note all aforementioned electrocatalysts were synthesized by the CTS method and tested in Li-O_2 battery configurations at two different current densities: (a) 200 mA/g_{carbon} and (b) 500 mA/g_{carbon}.

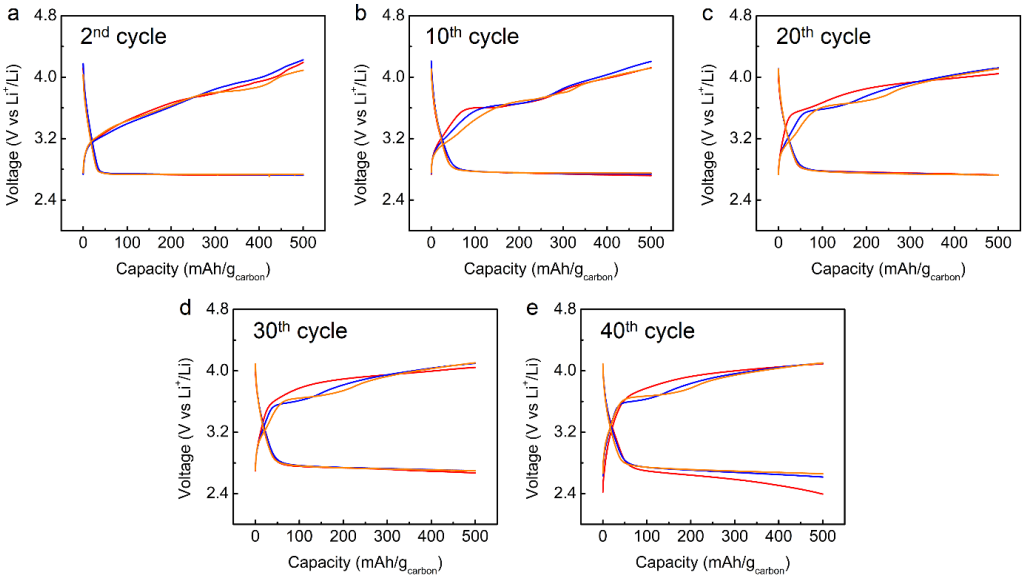

Figure S18. (a-e) Voltage profiles at specific cycle numbers for the binary (red), quaternary (blue) and octonary (orange) CTS nanoparticle-loaded 3DOm carbon cathodes. During Li-O_2 battery operation, no significant differences in terms of catalytic activity (other than capacity decay) can be observed for all aforementioned cathodes.

9. Product detection during Li-O_2 battery operation

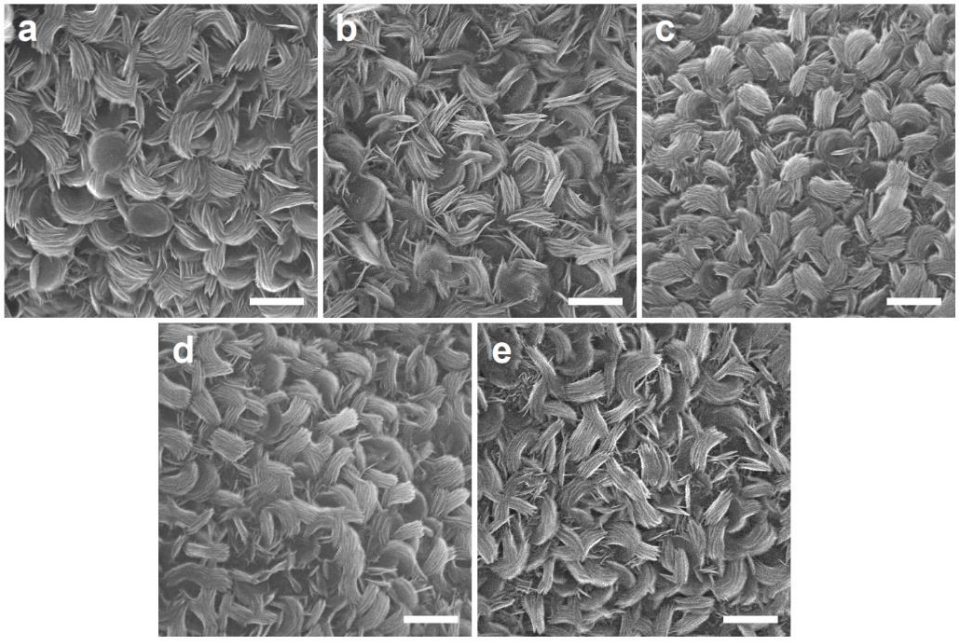

Figure S19. SEM images showing the discharge product morphologies (i.e. Li_2O_2) upon deep discharge for each Li-O_2 cathode: (a) bare 3DOm carbon, (b) WI RuIr, (c) CTS RuIr, (d) CTS RuIrCeNi, and (e) CTS RuIrCeNiWCuCrCo nanoparticle-decorated 3DOm carbon, respectively. Note the cells were discharged at 200 mA/g_{carbon} with a cutoff capacity of 3,000 mAh/g_{carbon}. Typical Li_2O_2 toroidal structures are observed across all tested samples with similar size/shape. Scale bar: 500 nm.

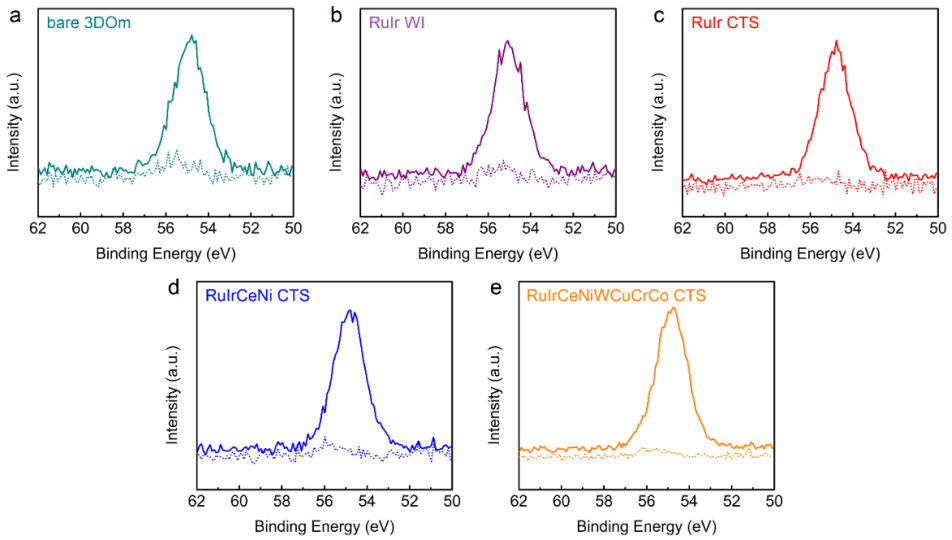

Figure S20. (a-e) The Li 1s XPS spectra for all 3DOm cathodes (bare to 8-element) in the discharged (solid line) and recharged (dashed line) states, corresponding to successful Li_2O_2 formation and decomposition respectively. The cells were discharged and then recharged at 200 mA/g_{carbon} with a 500 mAh/g_{carbon} cutoff capacity. The peak around 55 eV indicates the presence of Li_2O_2 particles on all discharged 3DOm cathodes regardless of nanoparticle (elemental) composition.

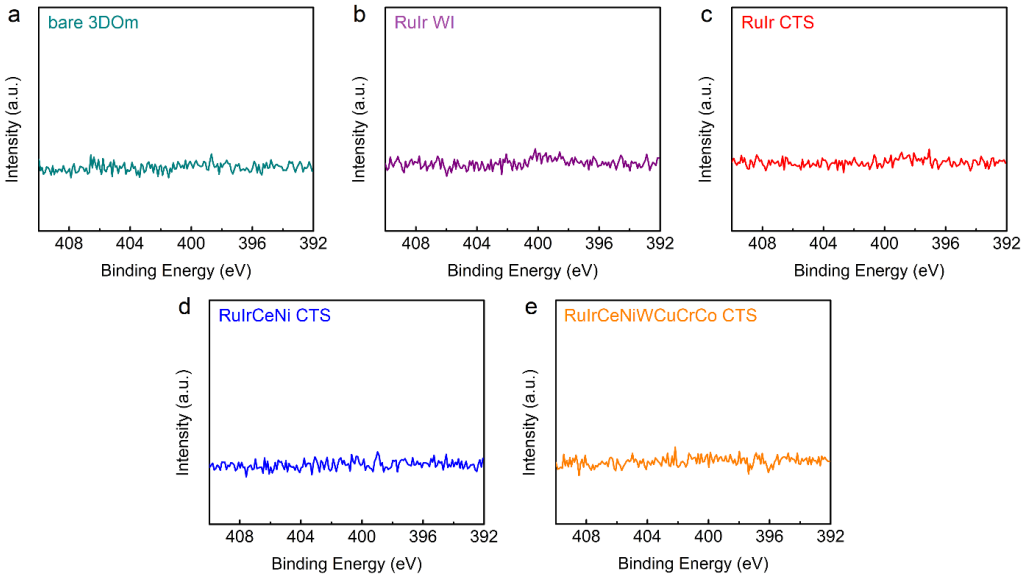

Figure S21. The N 1s XPS spectra for all discharged 3DOm cathodes: (a) bare, (b) WI RuIr, (c) CTS RuIr, (d) CTS RuIrCeNi, and (e) CTS RuIrCeNiWCuCrCo, respectively. This control data indicates that the Li signal shown in Figure S17 is not due to the presence of residual salt (LiTFSI) leftover after washing each cathode prior to XPS. Thus, the minimal N signal (and notable Li signal) unequivocally corresponds to Li_2O_2 present on the surface of each discharged cathode.

10. Elemental maps of the electrochemically cycled RuIrCeNi and RuIrCeNiWCuCrCo CTS nanoparticles on 3DOm carbon

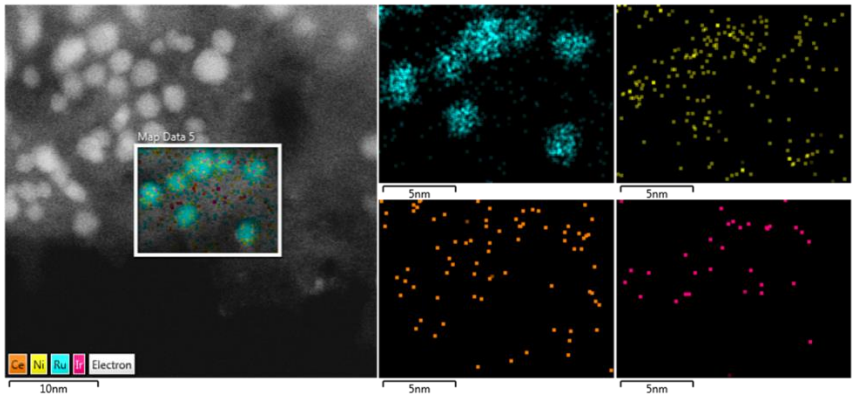

Figure S22. Overlay and individual elemental maps for the 4-element (RuIrCeNi) CTS nanoparticles on 3DOm after 20 electrochemical cycles

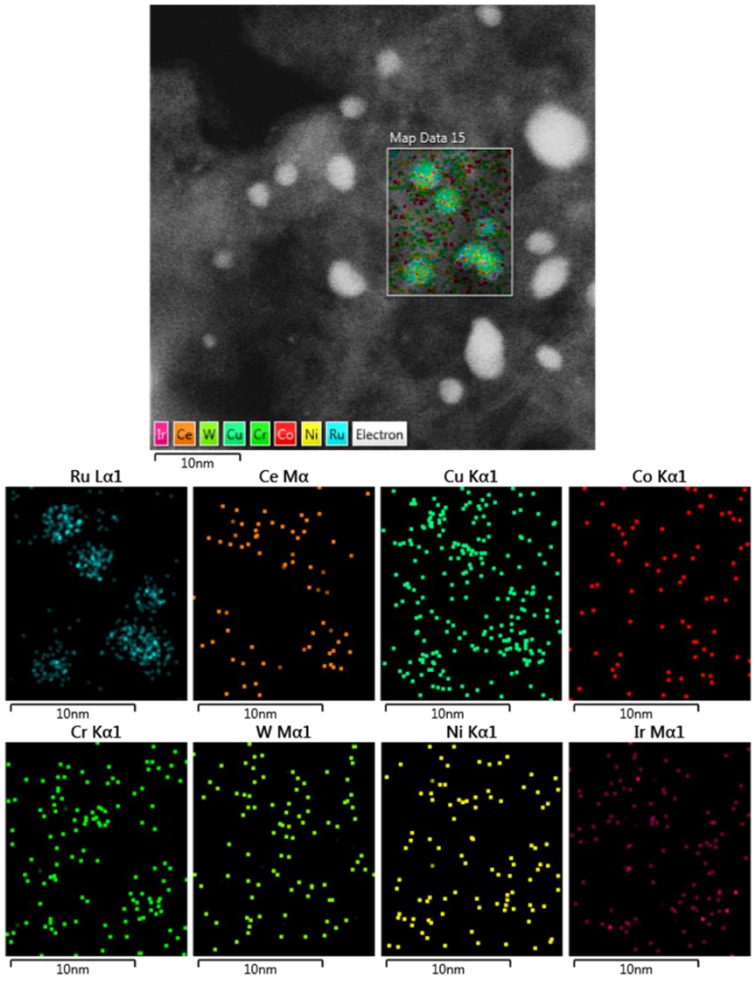

Figure S23. Overlay and individual elemental maps for the electrochemically cycled RuIrCeNiWCuCrCo nanoparticle-loaded 3DOm cathode.

11. Additional application of CTS nanoparticles on Vulcan substrates using a more stable water-in-salt (WiS) electrolyte

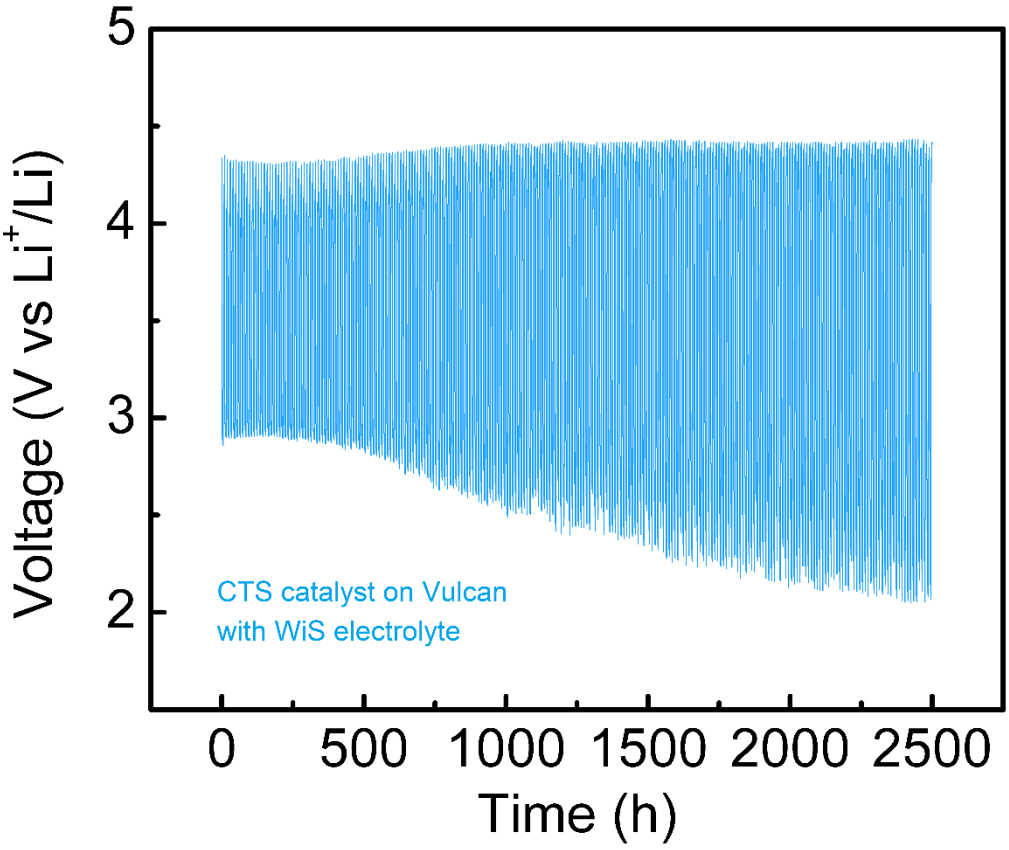

Figure S24. Cyclability of quaternary (RuIrCeNi) nanoparticles loaded onto commercial Vulcan carbon using WiS electrolyte at 50 mA/g_{carbon}. Compared to bare Vulcan Li-O_2 battery cathodes (ca. 70 cycles), these CTS-synthesized 4-element Vulcan cathode achieved >250 cycles without reaching the voltage limits (2V, 4.5V) with the same WiS electrolyte and overall cell conditions.

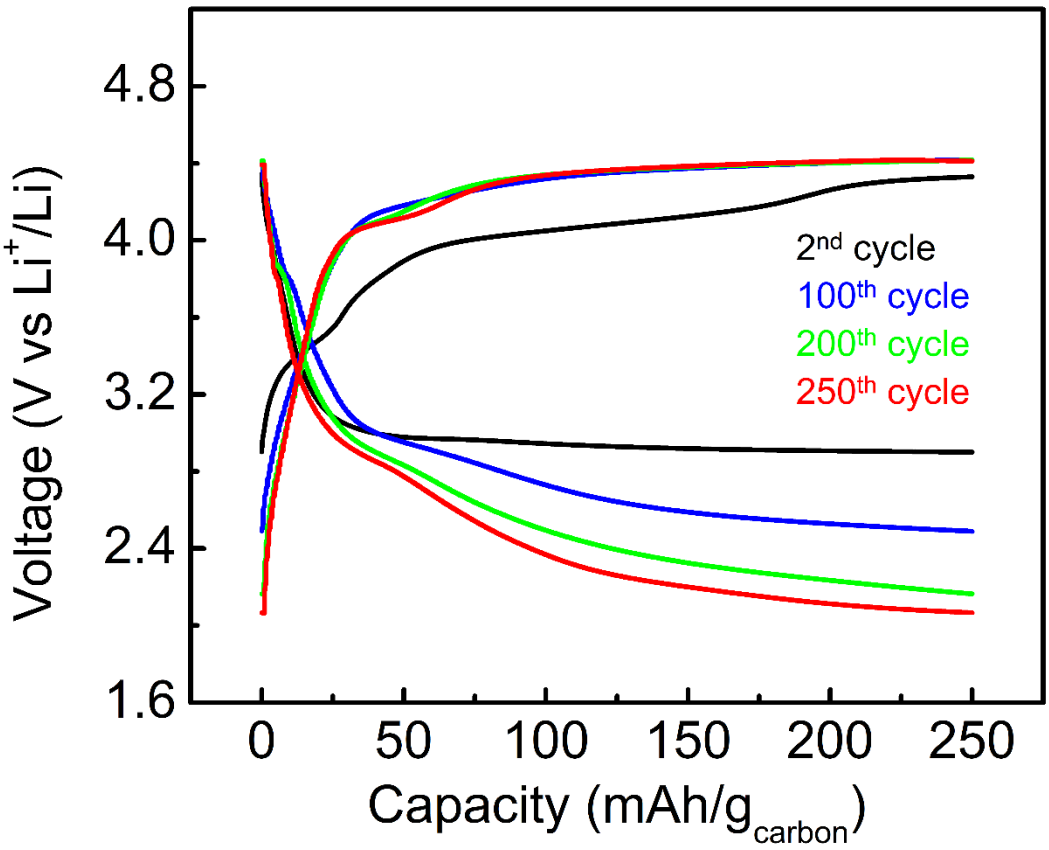

Figure S25. Detailed cycling plots for the RuIrCeNi/Vulcan WiS cathode. Although the overpotential continuously increases over hundreds of cycles, the cell remains within the set voltage window over prolonged Li-O_2 battery operation. Note that each cycle took 10 hours to complete at this cutoff capacity and current density (50 mA/g_{carbon}).

Reference

1. Fan, W.; Snyder, M. A.; Kumar, S.; Lee, P.-S.; Yoo, W. C.; McCormick, A. V.; Lee Penn, R.; Stein, A.; Tsapatsis, M. Hierarchical nanofabrication of microporous crystals with ordered mesoporosity. *Nat. Mater.* **2008**, *7*, 984.

2. Dong, Q.; Yao, X.; Zhao, Y.; Qi, M.; Zhang, X.; Sun, H.; He, Y.; Wang, D. Cathodically stable Li-O_2 battery operations using water-in-salt electrolyte. *Chem* **2018**, *4*, 1345−1358.

3. Yao, Y.; Huang, Z.; Xie, P.; Lacey, S. D.; Jacob, R. J.; Xie, H.; Chen, F.; Nie, A.; Pu, T.; Rehwoldt, M.; Yu, D.; Zachariah, M. R.; Wang, C.; Shahbazian-Yassar, R.; Li, J.; Hu, L. Carbothermal shock synthesis of high-entropy-alloy nanoparticles. *Science* **2018**, *359*, 1489−1494.

4. Xie, J.; Yao, X.; Cheng, Q.; Madden, I. P.; Dornath, P.; Chang, C.-C.; Fan, W.; Wang, D. Three dimensionally ordered mesoporous carbon as a stable, high-performance Li-O_2 battery cathode. *Angew. Chem. Int. Ed.* **2015**, *54*, 4299−4303.